Highlights of Spanish Astrophysics VIII, Proceedings of the XI Scientific Meeting of the Spanish Astronomical Society held on September 8–12, 2014, in Teruel, Spain. A. J. Cenarro, F. Figueras, C. Hernández-Monteagudo, J. Trujillo Bueno, and L. Valdivielso (eds.)

What is the progenitor of the Type Ia SN 2014J?

M. A. Pérez-Torres[1,2], P. Lundqvist[3,4], R. J. Beswick[5], C. I. Björnsson[3], T.W.B. Muxlow[5], Z. Paragi[6], S. Ryder[7], A. Alberdi[1], C. Fransson[3,4], J. M. Marcaide[8], I. Martí-Vidal[9], E. Ros[8,10], M. K. Argo[5] and J. C. Guirado[10,11]

[1] Instituto de Astrofísica de Andalucía, Glorieta de la Astronomía, s/n, E-18008 Granada, Spain.
[2] Centro de Estudios de la Fíísica del Cosmos de Aragón, E-44001 Teruel, Spain.
[3]Department of Astronomy, Stockholm University, SE-10691, Sweden.
[4]The Oskar Klein Centre, AlbaNova, SE-10691 Stockholm, Sweden.
[5]Jodrell Bank Centre for Astrophysics, University of Manchester, Oxford Road, Manchester.
[6]Joint Institute for VLBI in Europe, Postbus 2, 7990 AA Dwingeloo, NL.
[7]Australian Astronomical Observatory, P.O. Box 915, North Ryde, NSW 1670, Australia.
[8]Depto. de Astronomía i Astrofísica, Universidad de Valencia, E-46100 Burjassot, Valencia, Spain.
[9]Onsala Space Observatory, Chalmers University of Technology, SE-43992 Onsala, Sweden.
[10]Max-Planck-Institut für Radioastronomie, D-53121 Bonn, Germany.
[11]Observatorio Astronómico, Universidad de Valencia, E-46980 Paterna, Valencia, Spain.

Abstract

We report the deepest radio interferometric observations of the closest Type Ia supernova in decades, SN 2014J, which exploded in the nearby galaxy M 82. These observations represent, together with radio observations of SNe 2011fe, the most sensitive radio studies of a Type Ia SN ever. We constrain the mass-loss rate from the progenitor system of SN 2014J to $\dot{M} \lesssim 7.0 \times 10^{-10}$ $M_\odot\,yr^{-1}$ (for a wind speed of 100 km s^{-1}). Our deep upper limits favor a double-degenerate scenario–involving two WD stars–for the progenitor system of SN 2014J, as such systems have less circumstellar gas than our upper limits. By contrast, most single-degenerate scenarios, i.e., the wide family of progenitor systems where a red giant, main-sequence, or sub-giant star donates mass to a exploding white dwarf, are ruled out by our observations. The evidence from SNe 2011fe and 2014J points in the direction of a double-degenerate scenario for both.

1 Introduction

Type Ia SNe are the end-products of white dwarfs (WDs) with a mass approaching, or equal to, the Chandrasekhar limit, which results in a thermonuclear explosion of the star. While it is well acknowledged that the exploding WD dies in close binary systems, it is still unclear whether the progenitor system is composed of a C+O white dwarf and a non-degenerate star (single-degenerate scenario), or both stars are WDs (double-degenerate scenario). In the single-degenerate scenario, a WD accretes mass from a hydrogen-rich companion star before reaching a mass close to the Chandrasekhar limit and going off as supernova, while in the double-degenerate scenario, two WDs merge, with the more-massive WD being thought to tidally disrupt and accrete the lower-mass WD (see, e.g., [5] and references therein). This lack of knowledge makes it difficult to gain a physical understanding of the explosions, and to model their evolution, thus also compromising their use as distance indicators.

Radio and X-ray observations can potentially discriminate between the progenitor models of SNe Ia. For example, in all single-degenerate (SD) scenarios there is mass transfer from a companion, a significant amount of circumstellar gas is expected (e.g., [1]), and therefore a shock is bound to form when the supernova ejecta are expelled. The situation would then be very similar to circumstellar interaction in core-collapse SNe (see above), where the interaction of the blast wave from the supernova with its circumstellar medium results in strong radio and X-ray emission [2]. On the other hand, the double-degenerate (DD) scenario will not give rise to any circumstellar medium close to the progenitor system, and hence essentially no prompt radio emission is expected. Nonetheless, we note that the radio emission increases with time in the DD scenario, contrary to the SD scenario. This also opens the possibility for confirming the DD channel in Type Ia SNe via sensitive SKA observations of decades-old Type Ia SNe.

Table 1: Log of radio observations

Starting UT	T^a day	$t_{\rm int}$ hours	Array	ν GHz	$S_\nu{}^b$ μJy	$\mathrm{L}_{\nu,23}{}^c$	$\dot{M}_{-9}{}^d$
Jan 23.2	8.2	–	JVLA	5.50	12.0	1.8	0.7
Jan 24.4	9.4	–	JVLA	22.0	24.0	3.5	3.7
Jan 28.8	13.8	13.6	eMERLIN	1.55	37.2	5.5	1.2
Jan 29.5	14.5	14.0	eMERLIN	6.17	40.8	6.0	3.6
Feb 4.0	20.0	11.0	eEVN	1.66	32.4	4.7	1.7
Feb 19.1	35.0	10.0	eEVN	1.66	28.5	4.2	2.9

[a] Mean observing epoch (in days since explosion, assumed to be on Jan 15.0).
[b] 3σ flux density upper limits, in μJy.
[c] The corresponding 3σ spectral luminosity, in units of $10^{23}\,\mathrm{erg\,s^{-1}\,Hz^{-1}}$.
[d] Inferred 3σ upper limit to the mass-loss rate in units of $10^{-9} M_\odot\,\mathrm{yr}^{-1}$, for an assumed wind velocity of $100\,\mathrm{km\ s^{-1}}$ and for $\epsilon_{\rm B} = 0.1$ (see main text for details).

2 Radio observations of SN 2014J

We observed the type Ia SN 2014J with the electronic Multi Element Radio Interferometric Network (eMERLIN) at 1.6 and 6.2 GHz, and with the electronic European Very Long Baseline Interferometry Network (EVN) at a frequency of 1.7 GHz. We observed SN 2014J several times between 28 January 2014 and 19 February 2014. We show in Table 1 our log for the radio observations, whose full details are given in [6].

We discuss the radio emission from SNe Ia within a scenario of Type Ib/c SNe (see, e.g.,[3]) but, since we only have upper limits for the radio emission from SN 2014J, we will neglect energy losses for the relativistic electrons. The spectrum of the radio emission from those SNe follows the "Synchrotron Self-Absorption" (SSA) form, i.e., a rising power law with $\nu^{5/2}$ (low-frequency, optically thick regime), and a declining power law, ν^{α} (high frequency, optically thin regime), where α is assumed to be constant. For most well studied SNe, $\alpha \approx -1$ [3]. We assume that electrons are accelerated to relativistic energies, with a power law distribution, $dN/dE = N_0 E^{-p}$; where $E = \gamma m_e c^2$ is the energy of the electrons and γ is the Lorentz factor. For synchrotron emission, $\alpha = (p-1)/2$, which indicates that $p \approx 3$ should be used. We denote $\epsilon_{\rm B} = u_{\rm B}/u_{\rm th}$, where $u_{\rm B} = B^2/(8\pi)$ and $u_{\rm th}$ are the (post-shock) magnetic and thermal energy densities, respectively; and $\epsilon_{\rm rel} = u_{\rm rel}/u_{\rm th}$, where $u_{\rm rel}$ is the energy density of the relativistic particles, assumed for simplicity to be electrons. (See [6] for details of the modelling of the radio emission.)

Fig. 1 shows the predicted radio light curves of SN 2014J in M 82 in the case of a pre-supernova steady wind ($\rho_{\rm CSM} \propto r^{-2}$), which is expected in SD scenarios, for $\epsilon_{\rm B} = 0.01$ and 0.1. An almost perfect overlap between modeled light curves occurs for the combination $\dot{M} = 7.0 \times 10^{-10}\,{\rm M}_{\odot}\,{\rm yr}^{-1}$ and $\epsilon_{\rm B} = 0.1$, and $\dot{M} = 4.2 \times 10^{-9}\,{\rm M}_{\odot}\,{\rm yr}^{-1}$and $\epsilon_{\rm B} = 0.01$. The values of $\dot{M}/v_w$ for SN 2014J in Figure 1 are chosen so that the 5.50 GHz light curves go through the JVLA 3σ upper limit on day 8.2. The light curves for other frequencies lie below their corresponding upper limits. The second most constraining limit is from our 1.55 GHz eMERLIN observation on day 13.8, yielding $\dot{M} \lesssim 1.15\ (7.0) \times 10^{-9}\,{\rm M}_{\odot}\,{\rm yr}^{-1}$ for $\epsilon_{\rm B} = 0.1\ (0.01)$ and $v_w = 100$ km s^{-1}. We show in Table 1 upper limits for all data points.

3 The progenitor scenarios of Type Ia SNe

The power of radio interferometric observations lies in the fact that they are a perfect tracer of the mass-loss rate of the pre-supernova wind. In [6], we showed that the optically thin radio emission from SN 2014J, in the case of a steady wind is approximately

$$L_{\nu,{\rm thin}} \propto \epsilon_{\rm B}^{1.1} \left(\dot{M}/v_w\right)^{1.3}\ t^{-1.45}$$

If $\epsilon_{\rm B}$ is fixed, the luminosity tells us directly what is the value of $(\dot{M}/v_w)$. Therefore, if we plot in a graph $\dot{M}$ vs. v_w, we can constrain the SD progenitors for SN 2014J. This is exactly the purpose of Figure 2, where we have drawn, schematically, the regions of the $(\dot{M}/v_w)$ parameter space occupied by the most popular SD progenitor scenarios, which include, in decreasing order of mass-loss rate from the supernova progenitor, symbiotic systems, WDs

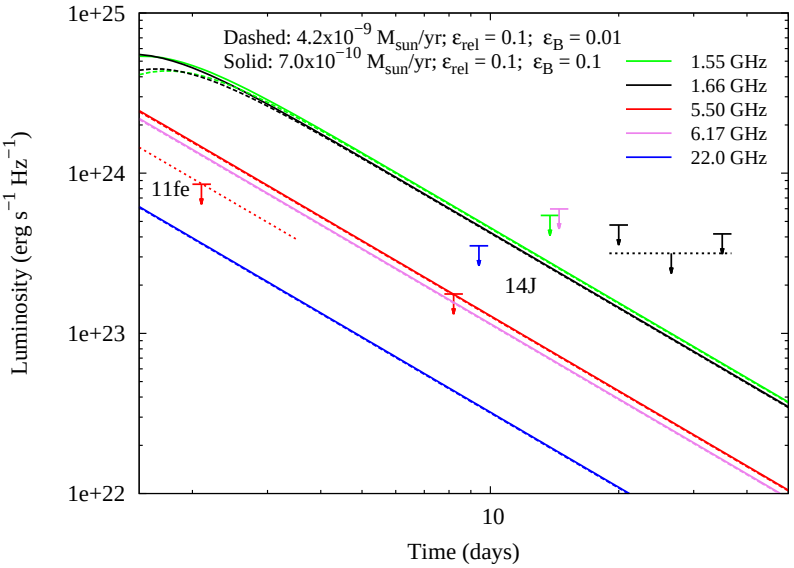

Figure 1: Predicted radio light curves of SN 2014J in M 82 for an assumed mass-loss rate of $\dot{M} = 7.0 \times 10^{-10}\,\mathrm{M}_\odot\,\mathrm{yr}^{-1}$(solid lines), and for $\dot{M} = 4.2 \times 10^{-9}\,\mathrm{M}_\odot\,\mathrm{yr}^{-1}$(dashed lines). For the former we used $\epsilon_\mathrm{B} = 0.1$ and for the latter $\epsilon_\mathrm{B} = 0.01$. The data points (cf. Table 1) with 3σ upper limits for SN 2014J are in the right part of the figure. Shown in the figure is also the earliest 5.9 GHz 3σ upper limit for SN 2011fe [4], scaled to its distance of 6.4 Mpc, together with a dotted line marking the predicted evolution for $\dot{M} = 5.0 \times 10^{-10}\,\mathrm{M}_\odot\,\mathrm{yr}^{-1}$(for $\epsilon_\mathrm{B} = 0.1$). Common parameters in all models are $\epsilon_\mathrm{rel} = 0.1$, $p = 3$ and $v_w = 100\,\mathrm{km\ s}^{-1}$. See text for further details.

with steady nuclear burning, and recurrent novae.

In a symbiotic system, the WD accretes mass from a giant star. The WD loses this accreted matter at rates of $\dot{M} \gtrsim 10^{-8}\,\mathrm{M}_\odot\,\mathrm{yr}^{-1}$and $v_w \approx 30\,\mathrm{km\ s}^{-1}$. The radio emission from those systems should have been detected by our deep sensitive observations. Thus, our radio non-detection rules out a symbiotic system as the progenitor of SN 2014J (red region in Figure 2).

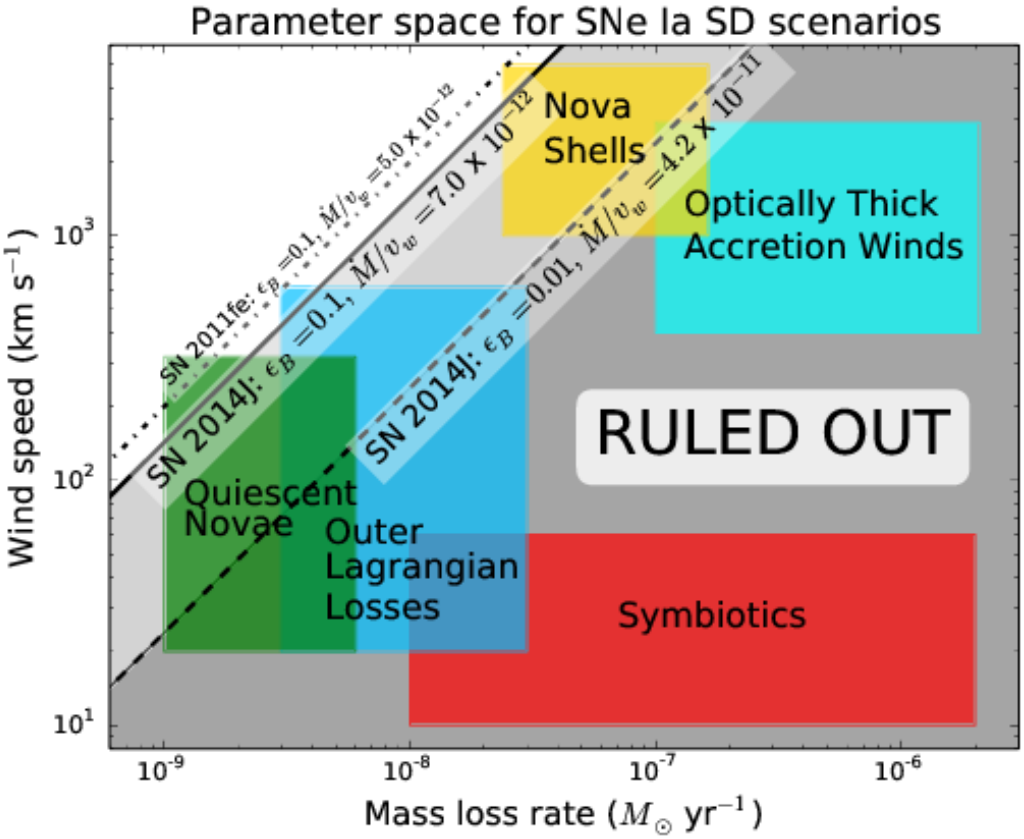

Figure 2: Constraints on the parameter space (wind speed vs. mass-loss rate) for SD scenarios for SN 2014J (see [6] for details). Progenitor scenarios are plotted as schematic zones, following [4]. We indicate our 3σ limits on $\dot{M}/v_w$, assuming $\epsilon_\mathrm{B} = 0.1$ (solid line) and the conservative case of $\epsilon_\mathrm{B} = 0.01$ (dashed line). Mass loss scenarios falling into the gray-shaded areas should have been detected by the deep radio observations, and therefore are ruled out for SN 2014J. For a comparison, we have included also the limit on SN 2011fe (dash-dotted line) for the same choice of parameters as the solid line for SN 2014J, which essentially leaves only room for quiescent nova emission as a viable alternative among the SD scenarios for SN 2011fe.

Another possible SD scenario is one where a main sequence, subgiant, helium, or giant star undergoes Roche lobe overflow onto the WD at rates of $3.1 \times 10^{-7}\,\mathrm{M}_\odot\,\mathrm{yr}^{-1} \lesssim \dot{M} \lesssim$

$6.7 \times 10^{-7}\,\mathrm{M}_\odot\,\mathrm{yr}^{-1}$. At those accretion rates, the WD experiences steady nuclear burning. For an assumed fraction $\epsilon_{\rm loss} = 0.01$ of the transferred mass to be lost from the system, the mass-loss rate is constrained to 3.1×10^{-9} $\mathrm{M}_\odot\,\mathrm{yr}^{-1} \lesssim \dot{M} \lesssim 6.7 \times 10^{-9}$ $\mathrm{M}_\odot\,\mathrm{yr}^{-1}$ and typical speeds of 100 km s$^{-1}\lesssim v_w \lesssim 3000$ km s^{-1}. At the lower end of $\dot{M}$, the mass loss through the outer Lagrangian points of the system proceeds at speeds up to $\sim$600 km s^{-1}. Most of the parameter space for the low-accretion rate scenario is ruled out by our radio observations, if $\epsilon_{\rm B} \simeq 0.1$ (blue region in Fig. 2). At the upper end of $\dot{M}$ the winds become optically thick, limiting the accretion rate to $\dot{M}_{\rm acc} \approx 6 \times 10^{-7}$ $M_\odot$ yr^{-1} and wind speeds of a few $\times$ 1000 km s^{-1}. Our data essentially rule out completely the high-accretion rate scenario of a WD with steady nuclear burning (cyan region in Fig. 2).

Finally, another possible SD channel is that of recurrent novae, which lie at the lowest accretion rate regime among popular SD scenarios. Here, a WD accreting at a rate $\dot{M} \approx (1-3) \times 10^{-7}$ $\mathrm{M}_\odot\,\mathrm{yr}^{-1}$, ejects shells of material at speeds of a few $\times 1000\,\mathrm{km\ s}^{-1}$, with typical recurrence times of a few years. The radio observations in Table 1 probe a radius of $\simeq (0.7-2.6) \times 10^{16}$ cm (for $s = 2$ and $\epsilon_{\rm B} = 0.1$), which constrains the presence of shells with recurrence times of $\lesssim 1.6$ $(v_{\rm shell}/2000$ km s$^{-1})^{-1}$ $(r_{\rm shell}/10^{16}$ cm) yr. Models of recurrent novae seem to indicate that as much as $\sim$15% of the accreted material over the recurrence time is ejected. For the typical accretion rates above, this implies an ejected shell mass of $\approx (2.4-7.1) \times 10^{-8}$ $M_\odot$, which should have been detected by our sensitive observations (see yellow region in Fig. 2). Unfortunately, the short duration of the nova radio burst, a few days at most, may have prevented its detection, so we cannot rule out completely the possibility of a nova shell ejection. During the quiescent phase between nova shell ejections, the WD accretes at a rate of $\dot{M} \sim 1 \times 10^{-7}$ $\mathrm{M}_\odot\,\mathrm{yr}^{-1}$, so that the mass-loss wind parameter is $\dot{M}/v_w \sim 1 \times 10^{-9}$ $(\epsilon_{\rm loss}/0.01)/100\,\mathrm{km\ s}^{-1}$. If $\epsilon_{\rm B} = 0.1$, our observations rule out almost completely the scenario with WD accretion during the quiescent phase of the star, whereas the case with $\epsilon_{\rm B} = 0.01$ cannot be excluded completely (green region in Fig. 2).

4 Summary

In summary, our observations exclude completely symbiotic systems and the majority of the parameter space associated with stable nuclear burning WDs, as viable progenitor systems for SN 2014J. Recurrent novae with main sequence or subgiant donors cannot be ruled out completely, yet most of their parameter space is also excluded by our observations. Therefore, our radio non-detections favour the DD scenario for SN 2014J.

Acknowledgments

The European VLBI Network (EVN) is a joint facility of European, Chinese, South African, and other radio astronomy institutes funded by their national research councils. The electronic Multi-Element Radio Linked Interferometer Network (eMERLIN) is the UK's facility for high resolution radio astronomy observations, operated by The University of Manchester for the Science and Technology Facilities Council (STFC). AA, JCG, JMM, MAPT, ER, and IMV acknowledge support from the Spanish MICINN through grants AYA2012-38491-C02-01 and AYA2012-38491-C02-02. P.L. acknowl-

edges support from the Swedish Research Council. The research leading to these results has received funding from the European Commission Seventh Framework Programme (FP/2007-2013) under grant agreement No 283393 (RadioNet3).

References

[1] Branch, D., Livio, M., Yungelson, L. R. et al. 1995, PASP, 107, 1019

[2] Chevalier, R. A. 1982, ApJ, 259, 302

[3] Chevalier, R. A., Fransson, C., Nymark, T. K. 2006, ApJ, 641, 1029

[4] Chomiuk, L., Soderberg, A. M., Moe, M., et al. 2012, ApJ, 750, 164

[5] Maoz, D., Mannucci, F., Nelemans, G. 2014, ARA&A, 52, 107

[6] Pérez-Torres, M. A., Lundqvist, P., Beswick, R. J., et al. 2014, ApJ, 792, 38